



This information is current as of July 17, 2017.

## Analysis of Celiac Disease Autoreactive Gut Plasma Cells and Their Corresponding Memory Compartment in Peripheral Blood Using High-Throughput Sequencing

Omri Snir, Luka Mesin, Moriah Gidoni, Knut E. A. Lundin, Gur Yaari and Ludvig M. Sollid

*J Immunol* 2015; 194:5703-5712; Prepublished online 13 May 2015;  
doi: 10.4049/jimmunol.1402611  
<http://www.jimmunol.org/content/194/12/5703>

---

<b>Supplementary Material</b>	<a href="http://www.jimmunol.org/content/suppl/2015/05/13/jimmunol.1402611.DCSupplemental">http://www.jimmunol.org/content/suppl/2015/05/13/jimmunol.1402611.DCSupplemental</a>
<b>References</b>	This article <b>cites 45 articles</b> , 16 of which you can access for free at: <a href="http://www.jimmunol.org/content/194/12/5703.full#ref-list-1">http://www.jimmunol.org/content/194/12/5703.full#ref-list-1</a>
<b>Subscription</b>	Information about subscribing to <i>The Journal of Immunology</i> is online at: <a href="http://jimmunol.org/subscription">http://jimmunol.org/subscription</a>
<b>Permissions</b>	Submit copyright permission requests at: <a href="http://www.aai.org/About/Publications/JI/copyright.html">http://www.aai.org/About/Publications/JI/copyright.html</a>
<b>Email Alerts</b>	Receive free email-alerts when new articles cite this article. Sign up at: <a href="http://jimmunol.org/alerts">http://jimmunol.org/alerts</a>



# Analysis of Celiac Disease Autoreactive Gut Plasma Cells and Their Corresponding Memory Compartment in Peripheral Blood Using High-Throughput Sequencing

Omri Snir,\* Luka Mesin,\*<sup>1</sup> Moriah Gidoni,<sup>†</sup> Knut E. A. Lundin,\*<sup>‡</sup> Gur Yaari,<sup>†,2</sup> and Ludvig M. Sollid\*<sup>2</sup>

Autoreactive IgA plasma cells (PCs) specific for the enzyme transglutaminase 2 (TG2) are abundant in the small intestine of patients with active celiac disease (CD), and their number drops in patients treated by dietary gluten elimination. Little is known about their characteristics and their role in the disease. In this study, using high-throughput sequencing of the IgH V region (IGHV) genes, we have studied features of TG2-specific PCs and their related B cell clones in peripheral blood. We found that TG2-specific PCs from both untreated and treated patients have acquired lower number of somatic hypermutation and used focused IGHV repertoire with overrepresentation of the *IGHV3-48*, *IGHV4-59*, *IGHV5-10-1*, and *IGHV5-51* gene segments. Furthermore, these PCs were clonally expanded and showed signs of affinity maturation. Lineage trees demonstrated shared clones between gut PCs and blood memory B cells, primarily IgAs. Some trees also involved IgG cells, suggesting that anti-TG2 IgA and IgG responses are related. Similarly to TG2-specific PCs, clonally related memory IgA B cells of blood showed lower mutation rates with biased usage of *IGHV3-48* and *IGHV5-51*. Such memory cells were rare in peripheral blood, yet detectable in most patients assessed by production of anti-TG2 Abs in vitro following stimulation of cells from patients who had been on a long-term gluten-free diet. Thus, the Ab response to TG2 in CD, while maintaining its IGHV gene usage, is dynamically regulated in response to gluten exposure with a low degree of maintenance at both PC and memory B cell levels in patients in remission. *The Journal of Immunology*, 2015, 194: 5703–5712.

In autoimmune diseases such as rheumatoid arthritis and lupus erythematosus, there is evidence that B cells play a central role in the pathogenesis (1–3). Disease-specific autoantibodies, produced by plasma cells (PCs) and/or plasmablasts, are commonly used in the clinic as diagnostic and prognostic biomarkers (4, 5). Likewise, in celiac disease (CD), a food-sensitive enteropathy with autoimmune features, IgA and IgG Abs reactive with transglutaminase 2 (TG2) are highly specific for CD (6). The accuracy of the serological assessment is so high that an additional evaluation of intestinal histology is no longer considered mandatory to make the diagnosis of CD in children (7). The anti-TG2 Ab response has two striking characteristics: 1) the Abs only occur in individuals who carry HLA-DQ2 or HLA-DQ8 (8), and 2) their production is entirely dependent on dietary gluten exposure (9, 10). A model where gluten-reactive T cells provide help to TG2-specific B cells by

means of hapten carrier-like gluten/TG2 complexes could explain these clinical observations (11).

IgA PCs that are specific for TG2 are highly abundant in the duodenal mucosa of CD patients when the disease is active, and their frequency decreases on commencement of a gluten-free diet (GFD) (12). Likewise, the titers of anti-TG2 Abs in serum drop dramatically within months after gluten is removed from the patients' diet, and the Ab levels correspond with the compliance of the GFD (10, 13). To what extent the anti-TG2 autoantibodies contribute to CD pathogenesis remains to be established (14). Studying the Ig repertoire of these autoreactive intestinal PCs and their unique features will be instrumental for the understanding of their role in the pathogenesis of CD.

Expression of Ig on the surface of intestinal IgA PCs facilitates visualization and capture of Ag-specific PCs (12, 15). Isolation of single TG2-specific PCs from the lesions of untreated CD patients and characterization of their Ig genes revealed a restricted repertoire with overrepresentation of IgH V region (*IGHV*)5-51 and *IGVK*1-5 gene segments, as well as limited somatic hypermutation (SHM) (12). Human mAbs (hmAbs) expression cloned from such PCs demonstrated that the Abs are not polyreactive (12) and specifically target conformational epitopes of TG2 that are clustered in the N-terminal part of the enzyme (12, 16). Four major epitopes could be identified, and the epitope reactivity of the hmAbs corresponded with the *IGHV* usage (12, 16). Most of the *IGHV*5-51 Abs react with epitope 1, whereas most of the *IGHV*3 and *IGHV*4 Abs react with epitopes 2 and 3, respectively (12, 16). Similar overrepresentation of *IGHV*5-51 gene had previously been observed among clones that were generated using phage display Ab libraries isolated from intestinal lymphocytes of CD patients (17).

The mucosal immune responses against T cell-dependent Ags show characteristics of secondary (i.e., memory) responses with rapid increase in the number of highly specific Abs toward the respective Ag upon rechallenge. Oral vaccination with cholera toxin

\*Centre for Immune Regulation and Department of Immunology, University of Oslo and Oslo University Hospital, 0372 Oslo, Norway; <sup>†</sup>Bioengineering Program, Faculty of Engineering, Bar-Ilan University, Ramat Gan 52900, Israel; and <sup>‡</sup>Department of Gastroenterology, Oslo University Hospital–Rikshospitalet, 0372 Oslo, Norway

<sup>1</sup>Current address: Whitehead Institute for Biomedical Research, Cambridge, MA.

<sup>2</sup>G.Y. and L.M.S. contributed equally to this work.

Received for publication October 14, 2014. Accepted for publication April 17, 2015.

This work was supported by European Research Council Grant ERC-2010-AdG-268541 and by a grant from the Research Council of Norway (to L.M.S.) as well as by a Bar-Ilan University Laboratory Establishment Grant to (G.Y.).

Address correspondence and reprint requests to Ludvig M. Sollid, Oslo University Hospital–Rikshospitalet, Sognsvannsveien 20, 0372 Oslo, Norway. E-mail address: l.m.sollid@medisin.uio.no

The online version of this article contains supplemental material.

Abbreviations used in this article: AP, alkaline phosphatase; CD, celiac disease; FR, framework region; gDNA, genomic DNA; GFD, gluten-free diet; hmAb, human mAb; HTS, high-throughput sequencing; IGHV, IgH V region; IMGT, ImMunoGeneTics; PC, plasma cell; SHM, somatic hypermutation; TG2, transglutaminase 2.

Copyright © 2015 by The American Association of Immunologists, Inc. 0022-1767/15/\$25.00

induces long-lived PCs in the lamina propria and memory B cells (18). Rotavirus memory B cells protect against reinfection via a mechanism that is dependent on the number of such cells in GALTs (19), and rotavirus-specific PCs could be isolated from the duodenum of subjects with no recent infection (15). These observations argue for the presence of gut PCs existing long after exposure to their Ags. In CD, TG2-specific PCs are present in the small intestine of many treated patients, which may suggest that some TG2-specific PCs are long-lived (12). The presence of these PCs could also be explained by a continuous, yet slow, influx of TG2-specific PCs emerging from a pool of memory B cells. Characterization of the TG2-specific PCs in treated CD patients paralleled by analysis of memory B cells in blood could shed light on this issue.

Whereas the characterization of Ig usage by single TG2-specific PCs gave valuable insight into anti-TG2 Ab characteristics, it gave information from few cells of a handful of patients, and only PCs of untreated patients were analyzed (12). To characterize the response in greater detail, also from treated CD patients, we have used high-throughput sequencing (HTS), which allows accurate in-depth investigation of the Ig sequence in a large number of cells (20). We performed comprehensive and comparative sequence analysis of the IGHV repertoire of PCs reactive or nonreactive with TG2 (i.e., TG2-specific or non-TG2-specific PCs) in untreated and treated CD patients as well as of B cells in peripheral blood of memory phenotype. We established that TG2-specific PCs are present in treated CD patients and that they share features of TG2-specific PCs from patients with active disease such as affinity maturation, clonal expansion, and overrepresentation of several IGHV genes. We identified rare TG2-related clones within the memory IgA pool and showed that they bear low number SHM and used an IGHV repertoire that is similar to their counterpart PCs in the gut. Furthermore, we demonstrated that such cells have the ability to produce anti-TG2 Abs upon stimulation. In light of these results, we suggest that autoimmunity against TG2 involves long-lived PCs whose persistence may have contribution from memory B cells.

## Materials and Methods

### Subjects and cells

Twenty patients with CD were enrolled in this study, 5 of whom were untreated and 15 who were treated with a GFD. All patients were diagnosed according to the guidelines of the American Gastroenterological Association. Clinicopathological information of the subjects is given in Tables I and II. IgA serum Ab levels specific for TG2 were determined by Celikey IgA, Varelisa (Thermo Scientific), and IgG serum Ab levels specific for deamidated gliadin were determined by Gliadin IgG II, DGP (Inova Diagnostics). Informed consent was obtained from all patients, and the study was approved by the Regional Ethics Committee of South-Eastern Norway (S-97201). PBMCs were isolated from blood collected in acid citrate dextrose tubes by density gradient centrifugation (Lymphoprep; Axis-Shield, Oslo, Norway). Gut biopsies of the duodenum obtained by endoscopy were kept in ice-cold RPMI 1640 (Life Technologies) before being transferred to RPMI 1640 supplemented with 2 mM EDTA and 3% FCS and subjected to continuous rotation for 1 h. Next, biopsies were digested with collagenase (1 mg/ml; Sigma-Aldrich, C-8051) in RPMI 1640 supplemented with 3% FCS for an additional hour in continuous rotation. Samples were then washed and single cells were collected following filtration through a 40- $\mu$ m cell strainer. PBMCs and single-cell suspensions from gut biopsies were cryopreserved until use.

### Isolating TG2-specific intestinal PCs and cDNA synthesis

Multimerized TG2 was used for sorting TG2-specific PCs. TG2 was expressed in Sf9 insect cells and BirA tag for site-specific biotinylation was added on its N terminus. To generate TG2 multimers, biotinylated TG2 was incubated with allophycocyanin-labeled streptamers (IBA) at a 4:1 molar ratio for 1 h in PBS supplemented with 3% FCS on ice. Single-cell suspensions from gut biopsies were then incubated with allophycocyanin-labeled TG2 streptamers for 45 min on ice. IgA-FITC (SouthernBiotech), Brilliant Violet 570 CD3 and CD14 (BioLegend), CD19-Pacific

Blue (BD Biosciences), and CD27-PE-Cy7 (eBioscience) were added for the last 20 min for staining of specific cellular lineage markers. IgA intestinal PCs were defined as live, large CD14/CD3-negative and highly expressed CD27. PCs were sorted for being either negative or positive for TG2 into 25  $\mu$ l catch buffer (i.e., 10 mM DTT and RNasin [2 U/ $\mu$ l; Promega] in PBS) and kept at  $-70^{\circ}\text{C}$  until cDNA synthesis. For cDNA synthesis, 1  $\mu$ g random hexamers (Roche), 0.45% (v/v) Nonidet P-40, and 1  $\mu$ l RNasin (40 U/ $\mu$ l; Promega) were added to 25  $\mu$ l sorted PCs extracts. Diethyl pyrocarbonate-treated water was added to final volume of 50  $\mu$ l and incubated at  $65^{\circ}\text{C}$  for 5 min and put on ice. Next, 20  $\mu$ l  $5\times$  RT buffer, 7  $\mu$ l DTT 100 mM, 9  $\mu$ l 10 mM dNTP mix (Promega), 1.5  $\mu$ l RNasin (40 U/ $\mu$ l; Promega), 1.8  $\mu$ l SuperScript III (Invitrogen), and 14  $\mu$ l diethyl pyrocarbonate-treated water were added. cDNA was synthesized at  $42^{\circ}\text{C}$  for 10 min,  $25^{\circ}\text{C}$  for 10 min,  $50^{\circ}\text{C}$  for 60 min, and  $94^{\circ}\text{C}$  for 5 min and stored at  $-20^{\circ}\text{C}$  until used.

### Sorting B cell subpopulations from peripheral blood and genomic DNA extraction

PBMCs were stained for 20 min at  $4^{\circ}\text{C}$  with Abs against the following Ags: IgA-FITC and IgG-PE (SouthernBiotech), CD3-PerCp, CD14-PerCp, CD19-Pacific Blue, and IgD-allophycocyanin (BD Biosciences), and CD27-PE-Cy7 (eBioscience) and B cell subpopulations were isolated using a FACSARIA cell sorter (BD Biosciences) according to subsequent experimental settings. The following B cell subsets were sorted for HTS: 1) innate memory IgD CD27 $^{+}$ , 2) memory IgA CD27 $^{+}$ , and 3) memory IgG CD27 $^{+}$ . Genomic DNA (gDNA) was purified from B cell subpopulations using the QIAamp DNA blood mini kit (Qiagen) according to the manufacturer's instructions. The following B cell subpopulations were sorted for Ab production analysis by ELISPOT and ELISA: 1) naive B cells IgD CD27 $^{-}$ , 2) innate memory IgD CD27 $^{+}$ , 3) switch IgA CD27 $^{-}$ , and 4) memory IgA CD27 $^{+}$ .

### HTS of IGHV genes

HTS of the IgH region from gDNA and cDNA was performed either as a commercial service on Illumina HiSeq platform as previously described (21) (Adaptive Biotechnologies) or on an Illumina MiSeq at the Norwegian Sequencing Centre in Oslo, Norway (<http://www.sequencing.uio.no>). The libraries for sequencing of the Illumina MiSeq platform were prepared in-house in the following way. The V<sub>H</sub> region was amplified from gDNA and cDNA using two sets of PCRs. Six forward primers, that is, V<sub>H</sub>1–6, from framework region (FR) 2 and one J region reverse primer were used for the first PCR (22, 23). Both forward and reverse primers included six unique nucleotides, which were used to index and thus combine different B cell subsets and PCs in a single sequencing library, followed by six random nucleotides and partial Illumina adapters (Supplemental Table I). First PCR was performed using AmpliTaq Gold polymerase (Applied Biosystems):  $95^{\circ}\text{C}$  for 7 min, 25 times  $95^{\circ}\text{C}$  for 30 s,  $60^{\circ}\text{C}$  for 45 s, and  $72^{\circ}\text{C}$  for 90 s, and  $72^{\circ}\text{C}$  for 10 min. A second PCR was set to complete Illumina MiSeq adapter sequences using Qiagen multiplex PCR:  $95^{\circ}\text{C}$  for 15 min, 10 times  $95^{\circ}\text{C}$  for 30 s,  $60^{\circ}\text{C}$  for 45 s, and  $72^{\circ}\text{C}$  for 90 s, and  $72^{\circ}\text{C}$  for 10 min. Final amplicon libraries were extracted from agarose gel (Qiagen) and paired-end sequencing of 250 bp was performed using Illumina MiSeq.

### Processing of raw sequencing data and alignment

The quality of raw reads was first evaluated using FastQC (<http://www.bioinformatics.babraham.ac.uk/projects/fastqc/>), and raw data were further processed using PRESTO (repertoire sequencing toolkit) (22) as previously described (24). In short, reads with a mean Phred quality of  $>20$  were removed, followed by removal of reads that did not contain sequencing primers. Reads were then assembled to a full sequence from FR2-J with an average length of 280 bp and collapsed to remove duplicated sequences. Only sequences that appeared in a single sample at least twice were used for further analysis. Sequences were then separated according to different sample indices. IGHV and IVHJ segments together with CDR3 were determined by the ImMunoGeneTics (IMGT) database (25).

IMGT as well as similar databases are likely to be incomplete (26–28); hence, nonreported polymorphisms are difficult to distinguish from somatic mutation in the IGHV alleles. We therefore created a personalized IGHV germline database for each patient. Such a database was constructed in two steps: 1) new alleles were discovered using a Tool for Ig Genotype Elucidation via Rep-Seq (28), and 2) realignment was accomplished using IgBLAST (29), as it can be modified and the personal reference repertoire can be used for alignment. Finally, IGHV gene usage and IGHV/IGHJ recombination were constructed using unique sequences, that is, considering one single representative read for each group of identical reads. The numbers of sorted cells that were used for HTS and unique sequences are given in Supplemental Table II.

Table I. Clinical information regarding patients that were analyzed by HTS

Patient	Gender	Age (y)	Years on GFD	Anti-Gliadin Titers	Anti-TG2 Titers	Marsh Score	HLA	Dietary Compliance
TCD628	F	60	22	<5	<1	1	DQ2.5	GFD, few incidents of gluten consumptions
TCD1086	M	54	>20	<5	<1	2	DQ2.5	GFD, Marsh score of 0 following 8 mo follow-up
TCD1140	F	54	16	<5	<1	0	DQ2.5	GFD, unspecific abdominal discomfort
TCD1170	F	27	26	<5	<1	0	DQ2.5	GFD, abdominal discomfort
TCD1131	M	48	20	<5	<1	0	DQ2.5	
UCD1141	F	66		>100	45.7	3c	ND	
UCD1182	M	27		29	9.6	3a	ND	
UCD1191	F	54		66	35.7	2	DQ2.5	
UCD1192	M	38		17	5.3	1	DQ2.5	
UCD1210	F	25		18	6.4	3b	DQ2.5	

TCD, treated CD patient; UCD, untreated CD patient.

*Clonal assignment between different subpopulations*

Clonally related sequences originate from a common ancestor. Functional V(D)J sequences from sorted memory B cell and PC subsets were assigned into clonal cluster based on the following criteria: 1) common IGHV/IGHJ gene segments and equal length of the junction region; and 2) following the first criteria, sequences differing from one another by a weighted distance <0.02 within the junction region were defined as clones. The distance between junction sequences was measured using the SSF mutability and substitution model (24). It follows that a threshold of 0.02 corresponds to 5–10 transition mutations or to 1–3 transversion mutations.

To account for variation in sampling size, the calculation of the frequency of clonal sharing between the different memory B cell subsets and PCs that are either TG2 specific or non-TG2 specific had been performed following multiple resampling of sequence data (100 times). Memory B cell subpopulations were randomly resampled according to the smallest memory B cell subset, whereas PCs were resampled according to the number of sequences in the TG2-specific subpopulation, which was the smallest in all patients. A hundred individual subdatasets were created accordingly for each patient. The frequency of shared memory B cells and PC clones was determined for each random dataset individually in two consecutive steps: 1) clonally related cells were first grouped according to the criteria that are given above within each subpopulation. The number of clones within each cell subpopulation is given in Supplemental Table II. 2) Next, we sought for clones that are shared between the different memory B cell subsets and PCs that were either non-TG2 specific or TG2 specific. Finally, the mean of the frequency of clonal sharing and 95% confidence interval of fractional error were calculated for a hundred individual tests.

The specificity of sorting TG2-specific PCs by TG2 mutimers is ~90%, and thus although being highly specific, false recognition of PCs for being negative or positive for TG2 may have occurred. Lavinder et al. (30) have recently demonstrated such error when sorting for tetanus toxoid plasma blast. To reduce the probability of such error, in clonal cluster where both TG2-specific and non-TG2-specific sequences were found, sequences were reassigned according to the majority of the original assignment.

*Generation of lineage trees*

Maximum parsimony lineage trees were generated for each clonal group containing at least one sequence from the gut and at least five total sequences. A single full-length, IMGT-numbered germline sequence was assigned to each clone using the IMGT germline reference database of IGHV and IGHJ gene sequences with a masked (replaced with Ns) D region. Duplicate sequences were then clustered, under the criteria that a sequence was a duplicate only when its full-length sequence was identical to another. This sequence was annotated as having been derived from all tissues within the cluster, and the copy number from each contributing sequence was summed to define the final copy number. Maximum parsimony lineages were inferred using the dnaps application of PHYLIP (31) using the germline sequence as the outgroup. This was followed by recursively replacing inferred ancestors in each tree with descendants having a Hamming distance of 0 from their inferred parent. Branch lengths were assigned as the Hamming distance between sequences, that is, the number of unambiguous mutation events.

*Diversity of B cell clone measurements*

Diversity for clones from TG2-specific and non-TG2-specific PCs as well as peripheral blood IgA B cells was calculated using the Hill diversity index, which measures diversity in a population (qD) as a smooth function of a single parameter ( $q$ ) (32, 33):

$$qD = \left( \sum_{i=1}^s p_i^q \right)^{1/(1-q)}$$

where  $s$  is the number of clones,  $p_i$  is the frequency of the  $i$  clone, and the parameter  $q$  determines how clonal frequencies are weighted (33).

Using the Hill diversity index, we determined whether the repertoire diversity as reflected by the clone size distribution differed between these subsets. To eliminate sampling effects, repertoires were subsampled (1000 times) according to the number of sequences in the smallest sample (i.e., the

Table II. Clinical information regarding patients that were analyzed by ELISPOT and ELISA

Patient	Gender	Age (y)	Years on GFD	Anti-Gliadin Titers	Anti-TG2 Titers	Marsh Score	HLA	Dietary Compliance
TCD494	M	54	12	<5	<1	0	DQ2.5	GFD
TCD838	F	41	2	21	<1	0	DQ2.5	GFD, abdominal discomfort, loose motions
TCD1072	F	23	12	<5	<1		ND	No information
TCD1092	F	52	41	6	<1	0	DQ2.5	GFD, drinks beer sometimes
TCD1099	F	25	15	12	<1	0	DQ2.5	GFD, takes oats and wheat starch, abdominal discomfort, loose motions
TCD1102	F	49	25	<5	<1	0	DQ9	GFD
TCD1103	F	49	11	<5	<1	0	DQ2.5	GFD
TCD1110	F	50	49	<5	<1	0	DQ2.5	GFD
TCD1120	F	67	22	<5	<1	0	DQ2.5	GFD
TCD1134	F	24	23	7	<2	0	DQ2.5	GFD
TCD1092	F	52	41	6	<1	0	DQ2.5	GFD, drinks beer sometimes

TCD, treated CD patient; UCD, untreated CD patient.

TG2-specific population), and the Hill curve was calculated in 1000 equally spaced  $q$  values between 0 and 15. At a given value of  $q$  ( $x$ -axis in Fig. 3), lower values of  $qD$  ( $y$ -axis) indicate lower diversity, that is, more focused repertoire. In the figure, the transparent bands from both sides of the main line indicate the middle 95% percentiles of the random samples; hence, statistical significance between samples can be visualized when lines are separated and fall outside of each other's bands.

#### *ELISPOT for detection and enumeration of TG2-specific IgA memory B cells*

B cells were sorted as described above to four different subpopulations: 1) naive B cells IgD CD27<sup>-</sup>, 2) innate memory IgD CD27<sup>+</sup>, 3) switch IgA CD27<sup>-</sup>, and 4) memory IgA CD27<sup>+</sup>. Non-B cells, that is, CD19<sup>-</sup> cells, were also collected and further used as feeder cells and negative control. Cells were cultured in 48-well plates ( $1.2 \times 10^6$  cells/well) and stimulated with a combination of *Staphylococcus aureus* Cowan I bacteria (1:10,000), PHA (2  $\mu$ g/ml), Con A (3  $\mu$ g/ml), and PWM (1/100,000) for 5 d as previously described (34). ELISPOT plates (Millipore) were coated overnight with 5  $\mu$ g/ml TG2 or anti-IgA (Sigma-Aldrich) at 4°C and further blocked with RPMI 1640 supplemented with 10% FCS at 37°C for 2 h. On day 5 cells were transferred to ELISPOT plates in 5 $\times$  consequence dilution and incubated overnight at 37°C, 5% CO<sub>2</sub>. Next, plates were washed six times with PBS supplemented with 0.05% Tween 20 followed by three washes with PBS. Alkaline phosphatase (AP)-conjugated anti-IgA (Sigma-Aldrich) was added and plates were incubated for 1 h at room temperature. Plates were developed using an AP-conjugated substrate kit (Bio-Rad) and bound Abs were counted with an S5 Versa ELISPOT analyzer (CTL, Bonn, Germany).

#### *ELISA for detection of IgA TG2-specific Abs*

ELISA assays was applied to monitor anti-TG2 Abs in supernatants from polyclonal-stimulated B cells in parallel to ELISPOT assay. Microtiter plates (Nunc, Roskilde, Denmark) were coated and incubated overnight at 4°C with TG2 at a concentration of 5  $\mu$ g/ml. Plates were then washed with PBS supplemented with 0.05% Tween 20 and blocked with 1% skimmed milk (Sigma-Aldrich) in PBS for 1 h. Following an additional wash, culture supernatants were transferred to plates and incubated for 2 h at room temperature. Plates were washed and anti-human IgA AP-conjugated (1:2000) (Sigma-Aldrich) was added and plates were incubated at room temperature. After 1 h of incubation plates were developed for ~10 min with phosphatase substrate (Sigma-Aldrich). Absorbance was measured at 405 nm.

#### *Statistical analysis*

Confidence intervals for VH gene usage analysis were estimated using the Wald method for log-frequency ratios. Statistical significance was determined using a proportion test after Yates continuity correction. The resulting  $p$  values were corrected for multiple testing using false discovery rates. Statistical significance for the difference in mutation load between TG2-specific and non-TG2-specific PCs was determined using a two-sided  $t$  test. A  $p$  value lower than  $\alpha = 0.05$  was considered statistically significant.

## **Results**

### *IGHV usage of TG2-specific PCs from untreated and treated CD patients*

Recent analysis of a limited number of single TG2-specific PCs from untreated CD patients revealed a limited and preferential IGHV segment usage (12). In this study, we wanted to comprehensively dissect the Ig gene repertoire of TG2-specific intestinal PCs of patients with active disease as well as of patients in remission using HTS. We determined the IGHV usage of TG2-specific PCs and compared this to the usage of non-TG2-specific PCs by calculating log-frequency ratios. The IGHV repertoire was markedly narrower in TG2-specific PCs compared with non-TG2-specific PCs, both in untreated and treated CD patients (Fig. 1A, 1B, Supplemental Fig. 1). In particular, *IGHV5-10-1* and *IGHV5-51* were significantly overrepresented in most of the untreated and treated CD patients (Table III). Biased usage was also seen for the *IGHV3* and *IGHV4* gene families, thus suggesting that TG2-specific Abs recognizing epitopes 2 and 3 were also represented among PCs analyzed (Fig. 1A, 1B, Table III). Patient CD628 was the only patient in which biased usage of *IGHV5* gene segments was not detected; instead, *IGHV4-59* and

*IGHV2-26* were overrepresented by TG2-specific PCs. Overrepresentation of *IGHV4-59* by TG2-specific PCs was detected in four additional patients, and *IGHV2-26*, which may target epitope 4, was also overrepresented by CD1210 (Table III). A schematic depiction of the IGHV genes that were used by all TG2-specific and non-TG2-specific PCs is shown in Fig. 1C. Of note, *IGHV3-48*, *IGHV4-59*, *IGHV5-10-1*, and *IGHV5-51* were commonly used.

We next studied whether there was a biased usage of IGHV genes in memory B cells of peripheral blood. IGH sequences were retrieved from three memory B cell subsets: 1) IgD CD27<sup>+</sup>, 2) IgA CD27<sup>+</sup>, and 3) IgG CD27<sup>+</sup>. Memory B cells were sorted from nine CD patients whose PC repertoires have already been established, and IGH genes were sequenced. The IGHV repertoires of the various memory B cell subsets demonstrated similarities with the repertoire used by the non-TG2-specific PCs, yet these were different from the biased repertoire used by the TG2-specific PCs (Fig. 1C, Supplemental Fig. 1).

IGHJ gene usage was similar between TG2-specific and non-TG2-specific PCs with few differences in expression of different JH genes. However there was no consistent pattern among patients (Supplemental Fig. 2).

### *Limited SHM in TG2-specific PCs from untreated and treated patients*

Previous analysis revealed that the IGHV genes used by TG2-specific PCs of untreated CD patients have limited SHMs (12). In this study, we investigated the number of mutations in IGHV sequences generated by HTS from untreated and treated patients. Sequences from untreated patients demonstrated a significantly lower rate of mutations in TG2-specific PCs compared with non-TG2-specific PCs (Fig. 2A). In treated CD patients, we also detected a lower degree of mutation even though the IGH region that was covered in the analysis of cells from those patients was relatively short (i.e., 110 bp, from FR3-J, Fig. 2B).

### *TG2-specific PCs have a low degree of diversity and are clonally expanded*

Evidence for clonally expanded PCs have been found both in human and mouse intestine (35–37). In the analysis of single TG2-specific PCs, two pairs of sister cells with identical Ig gene sequences were found among 36 single-sorted cells from one individual (12), suggestive of clonal expansion of gut TG2-specific PCs. We therefore wanted to investigate the relative size of TG2-specific clones and their diversity. To better understand the features of clonal expansions, we included in the analysis HTS data of peripheral blood IgA B cells of memory phenotypes. We used the Hill diversity index to summarize the properties of clone size distributions into one curve of  $qD$  values depicting the diversity of order, termed  $q$  (32, 33). When  $q = 0$ ,  $qD$  is the total number of clones. When  $q = 1$ ,  $qD$  is the Shannon entropy, and for very large values of  $q$ ,  $qD$  approaches the reciprocal of the frequency of the largest clone.  $qD$  values were established for TG2-specific, non-TG2-specific, as well as IgA cells of memory phenotype from each patient. To account for different sampling depth, sequences were subsampled multiple times according to the total number of TG2-specific sequences, which consistently were the smallest samples across all individuals. TG2-specific PCs had the lowest diversity in all patients, which was followed by non-TG2-specific PCs and memory IgA B cells, respectively (Fig. 3). The observed lower  $qD$  values of TG2-specific PCs indicate a lower number of clones in a given number of sequences, hence implying that TG2-specific PC clones are larger in size on average and clonally expanded.  $qD$  for larger values of  $q$  provides a second indication of clonal size, as the diversity is approaching the reciprocal of the frequency of the largest clone within

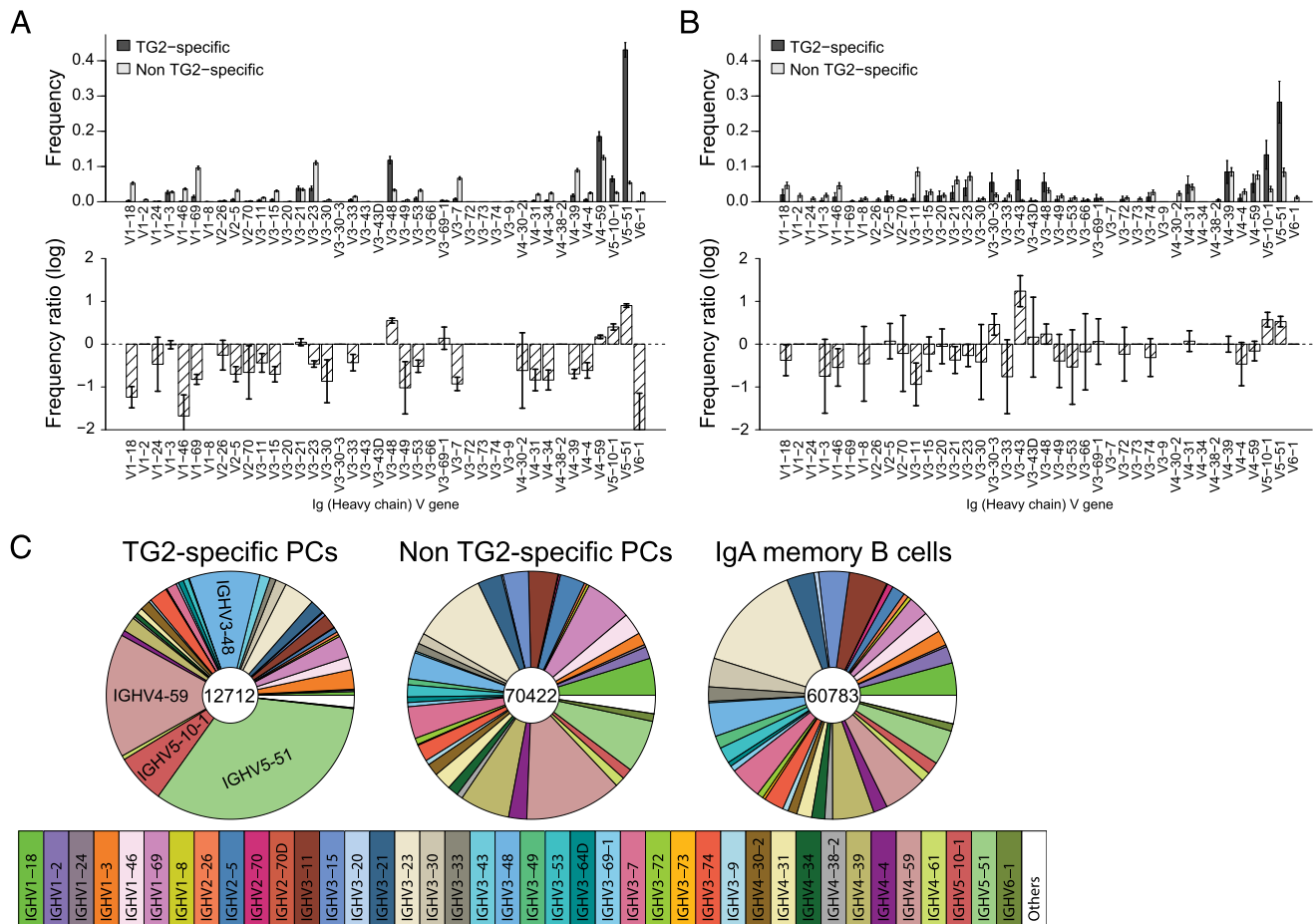


**FIGURE 1.** Preferential usage of IGHV genes by TG2-specific PCs. IGHV gene usage in two representative CD patients: (A) untreated and (B) treated. The frequencies of IGHV gene segments that were used by TG2-specific and non-TG2-specific PCs are shown in the upper panels. Log frequency ratios and 95% confidence interval for over-/underrepresentation of IGHV gene segments by TG2-specific PCs in comparison with non-TG2-specific TG2 PCs are shown in the lower panels. Significant overrepresentation of IGHV gene segments by TG2-specific is shown as positive log frequency ratios and confidence interval > 0. (C) Overview of the collective IGHV genes that were used by TG2-specific and non-TG2-specific PCs, as well as IgA memory B cells in all analyzed CD patients ( $n = 10$ ).

a certain population. In all patients, qD for  $q = 15$  (large enough for approaching the asymptotic value of qD) was found to be lowest for TG2-specific PCs (Fig. 3). Thus, TG2-specific PCs represent the largest clones within the sampled cell populations in all patients.

#### *Intestinal IgA immunity is clonally linked with the memory IgA compartment in blood*

The gut IgA system can recall previously selected PC clones from the memory B cell pool (37). Clonal relatedness between the gut mucosa and peripheral blood has been demonstrated in patients with ulcerative colitis (38). Similarly, clonally related B cells were found on both sides of the blood-brain barriers of patients with multiple sclerosis (39, 40). In the present study, we evaluated the degree of clonal relatedness between peripheral memory B cells of IgD, IgA, and IgG isotypes with IgA intestinal PCs that were either TG2 specific or nonspecific with TG2. Nine CD patients from whom we had IGH sequencing data from both PCs and peripheral memory B cells were included in the analysis. Following multiple resampling that was used to account for variation in samples size, unique sequences that originated from a common progenitor were clustered into clones within the five cell-sorted subgroups (i.e., TG2-specific/nonspecific PCs and the three memory B cell subsets), as previously described (24). Next, we calculated the frequency of clones that were shared between intestinal PCs that were either reactive or nonreactive with TG2 and memory B cells in peripheral blood.

Intestinal PCs, both TG2 specific or non-TG2 specific, were predominantly related to IgA memory B cell clones. PCs also shared clones with IgD and IgG memory B cells, albeit to a lesser extent (Fig. 4). Approximately 10% (4.7–14.9%) of non-TG2-specific PCs clones had related IgA memory B cell clones in peripheral blood. In comparison, the frequency of TG2-specific PCs that had related IgA B cell clones in peripheral blood was lower in most patients, with no visible differences between treated and untreated patients (ranging between 2.7 and 6.2%). In four patients the differences between the frequency of shared memory IgAs with non-TG2-specific and TG2-specific PC clones were statistically significant. In two patients, namely CD628 and CD1141, the frequencies of memory IgA clones that were shared with either TG2-specific or non-TG2-specific PCs were comparable.

#### *Clonal evolution of intestinal TG2-specific PCs*

To better understand the clonal evolution of gut PC clones and their clonal relatedness with memory B cells in blood, we generated 2368 lineage trees from clonal clusters with five or more unique sequences in which at least one IGHV sequence originated from either non-TG2-specific or TG2-specific PCs. Overall, the lineage trees showed two major patterns that were seen in trees representing both TG2-specific and non-TG2-specific PCs. One pattern consisted of complex and wide trees with a number of central branches close to the root of the trees, which narrowed as affinity matured by

Table III. IGHV genes that are overexpressed by TG2-specific PCs

Active Patient	Gene	<i>p</i> Value	FDR	Log Frequency Ratio and 95% Confidence Interval
UCD1141	IGHV1-69	<0.05	<i>p</i> = 0.09	0.42 (0.07–0.78)
	IGHV3-20	<0.01	<i>p</i> < 0.05	0.84 (0.24–1.45)
	IGHV3-43	<0.001	<i>p</i> < 0.001	0.46 (0.28–0.63)
	IGHV4-30-2	<0.05	<i>p</i> = 0.07	0.25 (0.04–0.46)
	IGHV4-34	<0.001	<i>p</i> < 0.01	0.46 (0.21–0.71)
	IGHV4-39	<0.01	<i>p</i> < 0.05	0.19 (0.06–0.31)
UCD1182	IGHV5-10-1	<0.05	<i>p</i> = 0.06	0.39 (0.09–0.69)
	IGHV5-51	<0.001	<i>p</i> < 0.001	0.39 (0.25–0.53)
	IGHV3-48	<0.001	<i>p</i> < 0.001	0.55 (0.49–0.61)
	IGHV4-59	<0.001	<i>p</i> < 0.001	0.17 (0.13–0.21)
	IGHV5-10-1	<0.001	<i>p</i> < 0.001	0.4 (0.33–0.47)
	IGHV5-51	<0.001	<i>p</i> < 0.001	0.9 (0.86–0.94)
UCD1191	IGHV4-59	<0.001	<i>p</i> < 0.001	0.36 (0.31–0.41)
	IGHV5-10-1	<0.001	<i>p</i> < 0.001	0.31 (0.18–0.43)
	IGHV5-51	<0.001	<i>p</i> < 0.001	0.74 (0.69–0.78)
UCD1192	IGHV3-30	<0.01	<i>p</i> < 0.05	0.22 (0.06–0.38)
	IGHV4-34	<0.01	<i>p</i> < 0.01	0.27 (0.09–0.46)
	IGHV4-59	<0.001	<i>p</i> < 0.001	0.12 (0.07–0.17)
	IGHV5-10-1	<0.001	<i>p</i> < 0.001	1.04 (0.96–1.12)
	IGHV5-51	<0.001	<i>p</i> < 0.001	0.75 (0.68–0.81)
UCD1210	IGHV1-3	<0.001	<i>p</i> < 0.001	0.82 (0.73–0.92)
	IGHV1-46	<0.001	<i>p</i> < 0.001	0.6 (0.51–0.69)
	IGHV2-26	<0.001	<i>p</i> < 0.001	1.03 (0.8–1.25)
	IGHV3-30	<0.001	<i>p</i> < 0.001	0.9 (0.77–1.03)
	IGHV3-33	<0.001	<i>p</i> < 0.001	0.45 (0.33–0.57)
	IGHV3-48	<0.001	<i>p</i> < 0.001	0.72 (0.67–0.77)
	IGHV3-74	<0.001	<i>p</i> < 0.001	0.44 (0.37–0.5)
	IGHV5-51	<0.001	<i>p</i> < 0.001	0.22 (0.17–0.27)
	IGHV2-26	<0.01	<i>p</i> = 0.07	1.07 (0.37–1.77)
	IGHV4-59	<0.01	<i>p</i> = 0.12	0.31 (0.08–0.55)
TCD1086	IGHV1-2	<0.001	<i>p</i> < 0.05	0.54 (0.2–0.87)
	IGHV1-46	<0.01	<i>p</i> < 0.05	0.32 (0.09–0.55)
	IGHV3-43D	<0.01	<i>p</i> < 0.05	1.30 (0.35–2.25)
TCD1131	IGHV5-10-1	<0.001	<i>p</i> < 0.001	0.57 (0.38–0.76)
	IGHV5-51	<0.001	<i>p</i> < 0.001	0.44 (0.29–0.59)
	IGHV1-69	<0.01	<i>p</i> = 0.06	0.37 (0.10–0.63)
	IGHV5-10-1	<0.001	<i>p</i> < 0.05	0.47 (0.19–0.75)
	IGHV5-51	<0.001	<i>p</i> < 0.001	0.55 (0.36–0.74)
TCD1140	IGHV3-30-3	<0.001	<i>p</i> < 0.01	2.31 (1.21–3.40)
	IGHV3-43	<0.001	<i>p</i> = 0.06	0.64 (0.16–1.13)
	IGHV5-10-1	<0.001	<i>p</i> < 0.001	2.83 (2.03–3.62)
	IGHV5-51	<0.001	<i>p</i> < 0.001	1.23 (1.05–1.41)
TCD1170	IGHV3-30-3	<0.01	<i>p</i> < 0.05	0.24 (0.06–0.41)
	IGHV3-43	<0.001	<i>p</i> < 0.001	0.98 (0.78–1.19)
	IGHV3-43D	<0.001	<i>p</i> < 0.001	0.91 (0.68–1.14)
	IGHV3-48	<0.001	<i>p</i> < 0.001	0.38 (0.21–0.56)
	IGHV4-30-2	<0.001	<i>p</i> < 0.001	0.19 (0.08–0.3)
	IGHV5-10-1	<0.001	<i>p</i> < 0.001	0.4 (0.23–0.57)
	IGHV5-51	<0.001	<i>p</i> < 0.001	0.71 (0.58–0.84)

FDR, false discovery rate; TCD, treated CD patient; UCD, untreated CD patient.

SHM. Fig. 5A depicts such a tree, which likely represents a process of robust affinity maturation against TG2. Another pattern consisted of narrow trees, generally with fewer mutations. This pattern, depicted in Fig. 5B, likely represents more focused selection. Among these, we observed trees that were solely composed of gut PCs. Such patterns were monitored both among non-TG2-specific and TG2-specific PC clones. Memory B cells could be missing from these trees due to inadequate sampling, or alternatively because PCs differentiate locally from B cells in the gut lamina propria. We also observed trees with memory B cells being situated at different positions in TG2-specific and non-TG2-specific trees, illustrating the existence of memory B cells in blood with either lower, parallel, or higher degree of maturation compared with their intestinal PC relative (Fig. 5C, 5D). Interestingly, in some trees we could find IgG memory B cells, thus linking the evolution of the IgG and IgA anti-TG2 responses (Fig. 5D).

#### Clonally related TG2-specific memory B cells show similar features to their intestinal PC counterpart

We further examined the Ig repertoire and the frequency of SHM in IGH that was acquired by memory IgA B cells that showed relatedness to TG2-specific PCs. Similarly to TG2-specific PCs, these IgA memory B cells expressed *IGHV3-48* and *IGHV5-51* at high frequencies and acquired lower number of SHM in comparison with memory cells that were related to TG2-specific clones (Fig. 6).

#### Functional analysis of TG2-specific IgA memory cells

The analysis of clonal relatedness between intestinal PCs and B cells in blood suggests that there exist infrequent IgA memory clones in blood that are TG2 specific. To substantiate this notion, we functionally examined for TG2-specific IgA memory cells in blood of treated CD patients by ELISPOT and ELISA. We sorted and isolated B cells from 10 patients of the following subpopulations: 1) naive

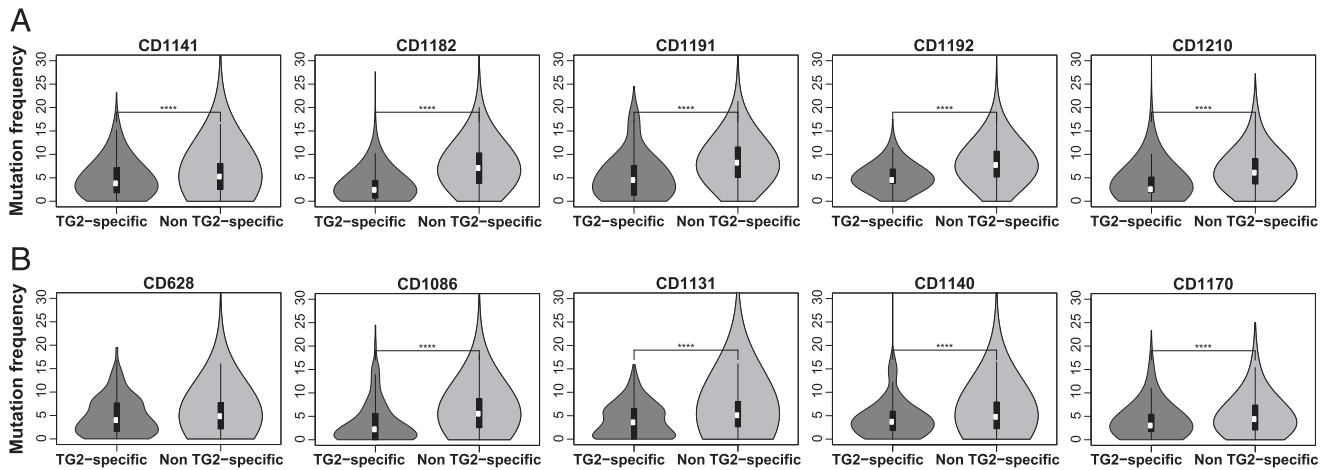


**FIGURE 2.** TG2-specific PCs demonstrate low levels of SHM. Comparison of the distributions of the frequency of SHM in the IgH genes of TG2-specific and non-TG2-specific PCs are shown in (A) untreated and (B) treated CD patients. \*\*\*\* $p < 0.0001$ .

IgD CD27<sup>-</sup>, 2) innate memory IgD CD27<sup>+</sup>, 3) switch IgA CD27<sup>-</sup>, and 4) memory IgA CD27<sup>+</sup>. Next, B cell subpopulations were stimulated polyclonally and anti-TG2 IgA secretion was monitored by ELISPOT following 5 d. Specific secretion of anti-TG2 Abs was predominantly detected from IgA B cells with memory phenotype, and their frequency ranged from 1/5000 to 1/500 TG2-specific cells of all IgA memory B cells (Fig. 7A). This range was in proximity to rates of shared IgA memory clones that were detected using HTS in blood of treated patients (0.1–0.5%). Importantly, IgA secretion was also detected from switched IgA CD27<sup>-</sup> and from innate memory IgD CD27<sup>+</sup> following 5 d of polyclonal stimulation. However, the levels of TG2-specific Abs were mostly at background levels. Additionally, the presence of anti-TG2 Abs was monitored in supernatants of stimulated cell cultures by anti-TG2 ELISA. Also in this study, anti-TG2 IgA Abs were specifically found in the supernatants of IgA memory cells and not in other B cell subpopulations (Fig. 7B).

## Discussion

Using a panel of hmAbs that were cloned and expressed from single-sorted TG2-specific PCs, we previously reported that anti-TG2 Abs use a restricted IGHV repertoire with limited SMH (12). Naturally, single-cell analysis set limits to the number of individuals and cells that were analyzed and may therefore provide insights to the most abundant TG2-reactive clones in the small intestine rather than characterizing such cells in an unbiased fashion. In the present study, we took the advantage of sorting TG2-specific PCs with high specificity and used HTS to overcome the limitation of the number of analyzed cells. Following such an in-depth analysis, we demonstrate that TG2-specific PCs from untreated CD patients as well as treated CD patients use a restricted IGHV repertoire with low diversity and primarily select for usage of particular VH genes. Furthermore, these autoreactive PC clones are expanded and have related clones in the periphery, predominantly within the IgA memory pool.

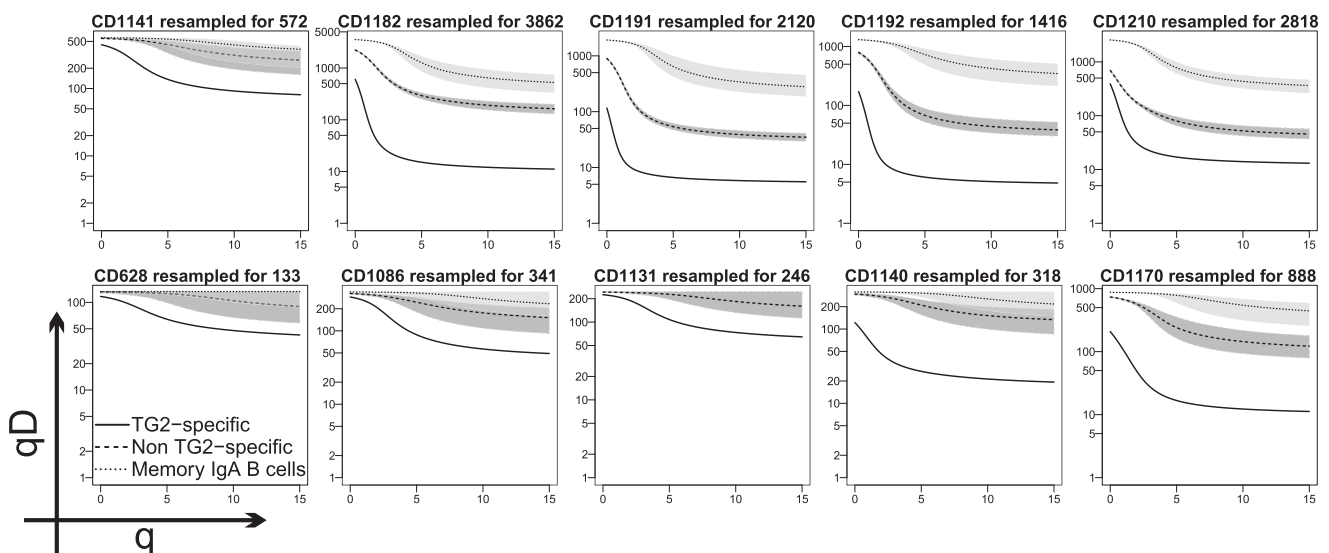
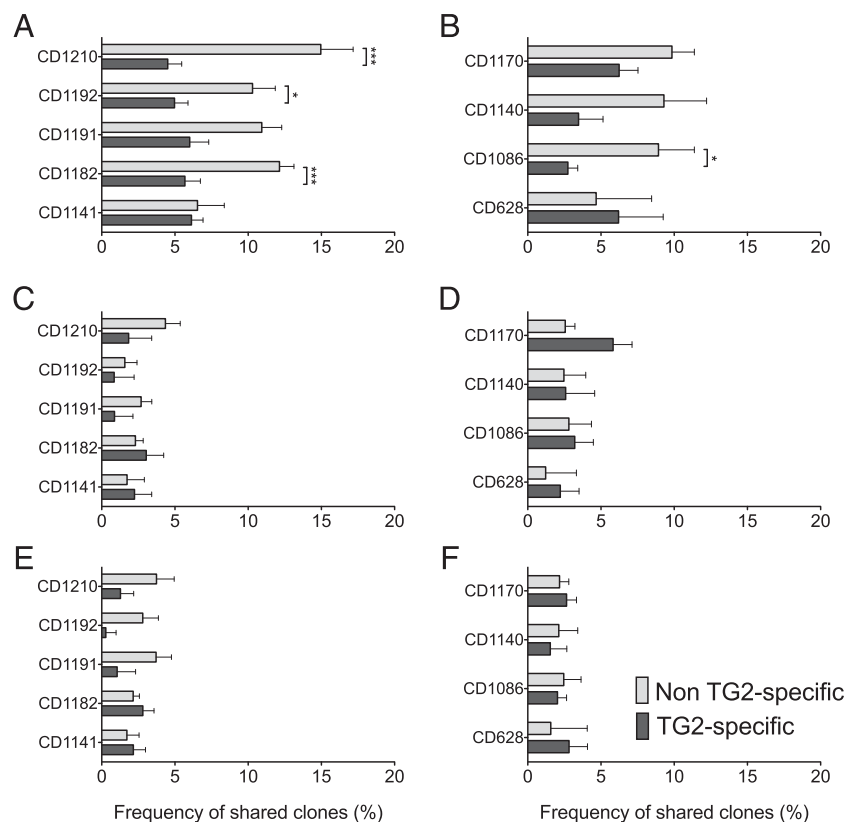


**FIGURE 3.** TG2-specific PCs have low diversity and are clonally expanded. Diversity and clonal size distribution of TG2-specific and non-TG2-specific PCs as well as peripheral blood IgA B cells of memory phenotype were measured by the Hill diversity index and compared. To eliminate the effect of sampling depth sequences from non-TG2-specific PCs and IgA memory B cells were randomly sampled 1000 times according to the number of unique sequences that were retrieved from the respective TG2-specific PC population. The number of resampled sequences for each patient is indicated in the figure. qD values depicted the level of diversity in a given value of q; lower qD values represent lower diversity. Transparent bands from both sides of the central lines indicate 95% percentiles. Differences between lines that are separated by an area >95% percentiles are significant. *Upper panels*, untreated CD patients; *lower panels*, treated CD patients.

**FIGURE 4.** Clonal relatedness between intestinal PCs and B cell subsets in peripheral blood. Unique sequences that were acquired from the following cell populations were clustered into clones within the respective subsets: 1) TG2-specific PCs, 2) non-TG2-specific PCs, 3) memory IgD CD27<sup>+</sup> B cells, 4) memory IgA CD27<sup>+</sup> B cells, and 5) memory IgG CD27<sup>+</sup> B cells. Clonal relatedness between PCs and memory B cell clones was further determined following clonal clustering between the different populations (see *Materials and Methods* for detailed description). Frequencies are shown of TG2-specific and non-TG2-specific PCs that had related memory B cell clones from peripheral blood of IgA isotype (**A** and **B**), IgD isotype (**C** and **D**), or IgG isotype (**E** and **F**) in untreated CD patient (*left panel*) and treated CD patients (*right panel*). \* $p < 0.05$ , \*\*\* $p < 0.001$ .



Intestinal IgA responses against T cell-dependent Ags usually evolve in germinal centers in gut-inductive sites and result in the formation of highly selected, affinity-matured PCs and long-lived memory cells (18, 41, 42). TG2-specific PCs likely develop with the help of T cells (12). Yet, the limited degree of Ab SHM suggests that they evolve extrafollicularly or in germinal center reactions of short duration (12). Of note, extrafollicular responses usually have less SHM but may give rise to memory B cells and long-lived PCs (43). Strikingly, in this work, we could monitor a distinguished population of TG2-specific PCs in patients who have been on a GFD >20 y, as well as in a patient who had been diagnosed in infancy and was on a GFD ever since (Table I). In light of these observations,

some intestinal TG2-specific PCs are either long-lived or are maintained by a slow and continuous influx of newly formed PCs from a memory pool. Our analysis, however, showed little clonal sharing between TG2-specific PCs and peripheral memory B cells in CD patients, either when the disease was active or in remission. If the gut PCs have a short life span, it is unlikely that replenishment of TG2-specific PCs by rare memory B cells alone can explain the maintenance of this cell population, particularly in the absence of stimulating Ag. Several reports argue that intestinal PCs that are generated in germinal centers are indeed long-lived, both in humans and in mice (15, 18, 44), and it could therefore be that some TG2-specific PCs are long-lived, possibly throughout the lifetime of patients.

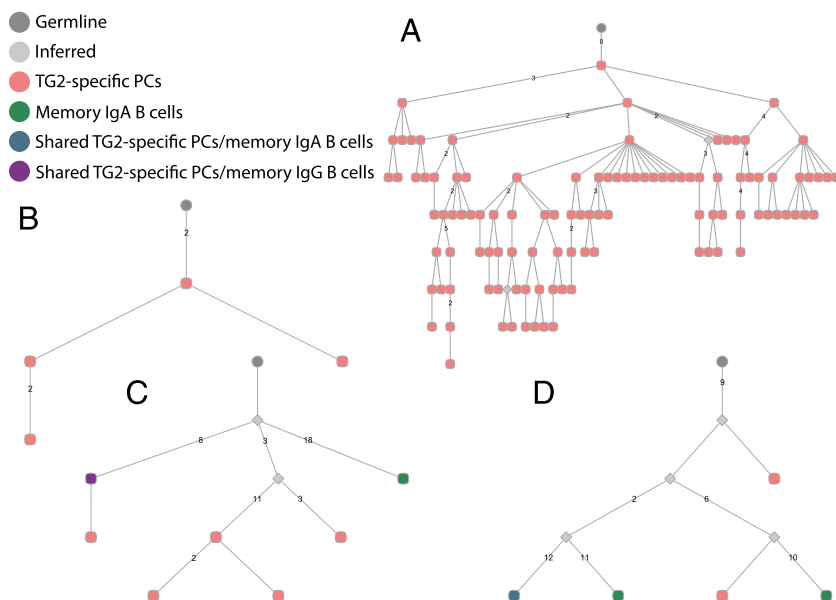
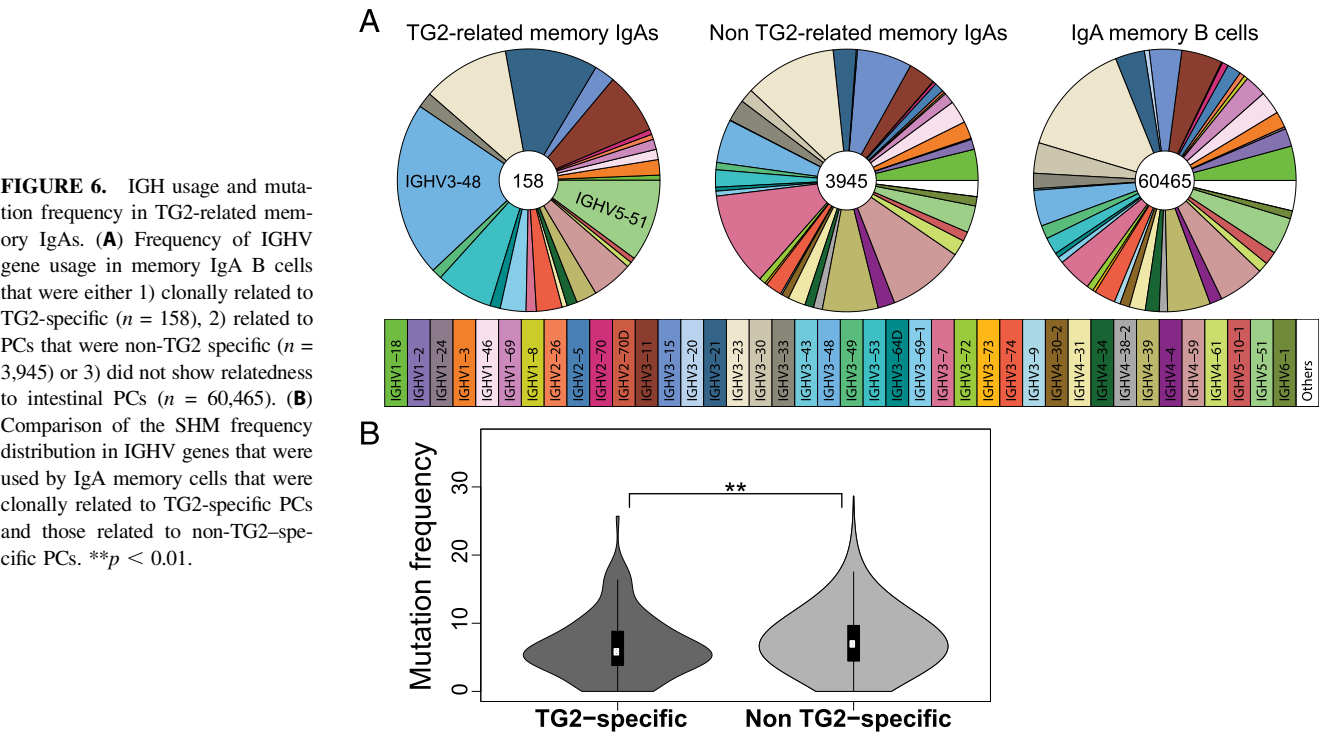


**FIGURE 5.** Differentiation and maturation of IgA intestinal PCs. Phylogenetic trees, which illustrate the evolution SHM in the IGHV gene of B cell clones from a putative germline sequence, were generated to all clusters of clones that include sequences from five cells or more with at least one PC sequence ( $n = 2368$ ). Representative trees for the two main lineage patterns that were found are depicted: (**A**) a large complex tree and (**B**) a focused tree of limited size. Memory B cells were found in many trees and located either higher in the trees compared with most PCs (**C**) or in parallel at the bottom of trees (**D**). IgG memory was also detected in a small number of trees (**C**).



Using phylogenetic trees, we could follow PC clones and visualize the nature of relatedness between cells from blood and the small intestine. We found memory IgA B cells in different evolutionary phases, and, interestingly, in some TG2-specific trees we found both IgA and IgG memory B cells, which suggests that some clones may have started developing from a common ancestor that further matured as IgA and IgG anti-TG2 Ab-producing cells. It has been demonstrated that B cells with different isotypes may share a common progenitor and are therefore clonally related (38, 45). Indeed, both IgG and IgA anti-TG2 Abs are found in sera of CD patients with an active disease. However, very few, if any, TG2-specific IgG PCs are present in the intestinal mucosa of untreated CD patients (12). A detailed proteomics analysis of serum IgG and IgA and mucosal IgA anti-TG2 Abs in combination with HTS of IGH of intestinal TG2-specific PCs are needed to validate the relationship between the different isotypes and how interrelated the Ab response is in gut mucosa and serum.

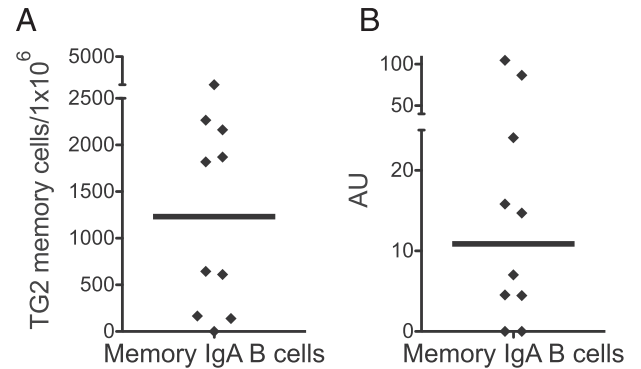


**FIGURE 7.** Peripheral memory IgA B cells produces anti-TG2 Abs upon stimulation. **(A)** Number of IgA anti-TG2-producing cells per million IgA memory B cells that were detected by ELISPOT following polyclonal stimulation. Cells were collected and sorted from 10 well-treated CD patients and stimulated for 5 d. **(B)** Detection of secreted anti-TG2 IgA Abs in the supernatants of the stimulated IgA memory B cell cultures. AU, arbitrary units.

The comprehensive analysis of a population of TG2-specific PCs in multiple untreated CD patients confirms and extends the view that was indicated by a limited analysis of single PCs from four untreated CD patients (12, 16). We found that TG2-specific PCs have lower numbers of SHM in their VH genes compared with non-TG2-specific PCs and they overexpress the *IGHV5-51* gene segment. These two features were also found in TG2-specific PCs from treated patients. Furthermore, we found that *IGHV5-10-1* as well as *IGHV3* and *IGHV4* genes were overrepresented by TG2-specific PCs and their clonally related memory IgA B cells. *IGHV3* and *IGHV4* are used by TG2-specific hmAbs that target epitopes 2 and 3 of TG2 (12, 16), thus suggesting that in addition to epitope 1 targeted by *IGHV5-51*-carrying Abs, epitopes 2 and 3 were also targeted by PCs of the patients included in this study. Overall, the IGHV repertoire that is used by TG2-specific PCs is limited and appears to be directed against a few epitopes of TG2.

Dominant, expanded PC clones that are synchronized in inductive sites in the GALT are a feature of the intestinal IgA response to oral immunization with T cell-dependent Ags (42), and they were also described in healthy intestine (37). In this study, using the Hill diversity index, we not only demonstrate that TG2-specific PCs have a focused repertoire with low diversity, but we also show that among the TG2-specific PCs few clones dominate. The dominance of several clones speaks to a concerted action in the course of the response, likely taking place in organized lymphoid tissue.

In summary, we have found that the Ab response to TG2 in CD is dynamically regulated in response to gluten exposure with low-degree maintenance at both PC and memory B cell levels in patients in remission. A key question for future research will be to determine how this infrequent, but persistent population of TG2-specific PCs in the gut lamina propria is maintained in CD patients even after years on a gluten-free diet.

### Acknowledgments

We thank Vikas K. Sarna for help in clinical assessment of CD patients.

## Disclosures

The authors have no financial conflicts of interest.

## References

- Chatzidionysiou, K., E. Lie, E. Nasonov, G. Lukina, M. L. Hetland, U. Tarp, C. Gabay, P. L. van Riel, D. C. Nordström, J. Gomez-Reino, et al. 2011. Highest clinical effectiveness of rituximab in autoantibody-positive patients with rheumatoid arthritis and in those for whom no more than one previous TNF antagonist has failed: pooled data from 10 European registries. *Ann. Rheum. Dis.* 70: 1575–1580.
- Jónsdóttir, T., I. Gunnarsson, A. Risselada, E. W. Henriksson, L. Klareskog, and R. F. van Vollenhoven. 2008. Treatment of refractory SLE with rituximab plus cyclophosphamide: clinical effects, serological changes, and predictors of response. *Ann. Rheum. Dis.* 67: 330–334.
- Jónsdóttir, T., A. Zickert, B. Sundelin, E. W. Henriksson, R. F. van Vollenhoven, and I. Gunnarsson. 2013. Long-term follow-up in lupus nephritis patients treated with rituximab—clinical and histopathological response. *Rheumatology (Oxford)* 52: 847–855.
- Aletaha, D., T. Neogi, A. J. Silman, J. Funovits, D. T. Felson, C. O. Bingham, III, N. S. Birnbaum, G. R. Burmester, V. P. Bykerk, M. D. Cohen, et al. 2010. 2010 Rheumatoid arthritis classification criteria: an American College of Rheumatology/European League Against Rheumatism collaborative initiative. *Arthritis Rheum.* 62: 2569–2581.
- Shiboski, S. C., C. H. Shiboski, L. Criswell, A. Baer, S. Challacombe, H. Lanfranchi, M. Schjodt, H. Umehara, F. Vivino, Y. Zhao, et al; Sjögren's International Collaborative Clinical Alliance (SICCA) Research Groups. 2012. American College of Rheumatology classification criteria for Sjögren's syndrome: a data-driven, expert consensus approach in the Sjögren's International Collaborative Clinical Alliance cohort. *Arthritis Care Res. (Hoboken)* 64: 475–487.
- Rostom, A., C. Dubé, A. Cranney, N. Saloojee, R. Sy, C. Garrity, M. Sampson, L. Zhang, F. Yazdi, V. Mamaladze, et al. 2005. The diagnostic accuracy of serologic tests for celiac disease: a systematic review. *Gastroenterology* 128(4, Suppl. 1): S38–S46.
- Husby, S., S. Koletzko, I. R. Korponay-Szabó, M. L. Mearin, A. Phillips, R. Shamir, R. Troncone, K. Giersiepen, D. Branski, C. Catassi, et al; ESPGHAN Working Group on Coeliac Disease Diagnosis; ESPGHAN Gastroenterology Committee; European Society for Pediatric Gastroenterology, Hepatology, and Nutrition. 2012. European Society for Pediatric Gastroenterology, Hepatology, and Nutrition guidelines for the diagnosis of coeliac disease. *J. Pediatr. Gastroenterol. Nutr.* 54: 136–160.
- Björck, S., C. Brundin, E. Lörcin, K. F. Lynch, and D. Agardh. 2010. Screening detects a high proportion of celiac disease in young HLA-genotyped children. *J. Pediatr. Gastroenterol. Nutr.* 50: 49–53.
- Dieterich, W., E. Laag, H. Schöpper, U. Volta, A. Ferguson, S. Gillett, E. O. Riecken, and D. Schuppan. 1998. Autoantibodies to tissue transglutaminase as predictors of celiac disease. *Gastroenterology* 115: 1317–1321.
- Sulkanen, S., T. Halttunen, K. Laurila, K. L. Kolho, I. R. Korponay-Szabó, A. Sarnesto, E. Savilahti, P. Collin, and M. Mäki. 1998. Tissue transglutaminase autoantibody enzyme-linked immunosorbent assay in detecting celiac disease. *Gastroenterology* 115: 1322–1328.
- Sollid, L. M., O. Molberg, S. McAdam, and K. E. Lundin. 1997. Autoantibodies in coeliac disease: tissue transglutaminase—guilt by association? *Gut* 41: 851–852.
- Di Niro, R., L. Mesin, N. Y. Zheng, J. Stamnaes, M. Morrissey, J. H. Lee, M. Huang, R. Iversen, M. F. du Pré, S. W. Qiao, et al. 2012. High abundance of plasma cells secreting transglutaminase 2-specific IgA autoantibodies with limited somatic hypermutation in celiac disease intestinal lesions. *Nat. Med.* 18: 441–445.
- Nachman, F., E. Sugai, H. Vázquez, A. González, P. Andrenacci, S. Niveloni, R. Mazure, E. Smecuol, M. L. Moreno, H. J. Hwang, et al. 2011. Serological tests for celiac disease as indicators of long-term compliance with the gluten-free diet. *Eur. J. Gastroenterol. Hepatol.* 23: 473–480.
- Sollid, L. M., and B. Jabri. 2013. Triggers and drivers of autoimmunity: lessons from coeliac disease. *Nat. Rev. Immunol.* 13: 294–302.
- Di Niro, R., L. Mesin, M. Raki, N. Y. Zheng, F. Lund-Johansen, K. E. Lundin, A. Chappillienne, D. Poncet, P. C. Wilson, and L. M. Sollid. 2010. Rapid generation of rotavirus-specific human monoclonal antibodies from small-intestinal mucosa. *J. Immunol.* 185: 5377–5383.
- Iversen, R., R. Di Niro, J. Stamnaes, K. E. Lundin, P. C. Wilson, and L. M. Sollid. 2013. Transglutaminase 2-specific autoantibodies in celiac disease target clustered, N-terminal epitopes not displayed on the surface of cells. *J. Immunol.* 190: 5981–5991.
- Marzari, R., D. Sblattero, F. Florian, E. Tongiorgi, T. Not, A. Tommasini, A. Ventura, and A. Bradbury. 2001. Molecular dissection of the tissue transglutaminase autoantibody response in celiac disease. *J. Immunol.* 166: 4170–4176.
- Lycke, N., and J. Holmgren. 1987. Long-term cholera antitoxin memory in the gut can be triggered to antibody formation associated with protection within hours of an oral challenge immunization. *Scand. J. Immunol.* 25: 407–412.
- Moser, C. A., and P. A. Offit. 2001. Distribution of rotavirus-specific memory B cells in gut-associated lymphoid tissue after primary immunization. *J. Gen. Virol.* 82: 2271–2274.
- Georgiou, G., G. C. Ippolito, J. Beausang, C. E. Busse, H. Wardemann, and S. R. Quake. 2014. The promise and challenge of high-throughput sequencing of the antibody repertoire. *Nat. Biotechnol.* 32: 158–168.
- Larimore, K., M. W. McCormick, H. S. Robins, and P. D. Greenberg. 2012. Shaping of human germ-line IgH repertoires revealed by deep sequencing. *J. Immunol.* 189: 3221–3230.
- van Dongen, J. J., A. W. Langerak, M. Brüggemann, P. A. Evans, M. Hummel, F. L. Lavender, E. Delabesse, F. Davi, E. Schuurink, R. García-Sanz, et al. 2003. Design and standardization of PCR primers and protocols for detection of clonal immunoglobulin and T-cell receptor gene recombinations in suspect lymphoproliferations: report of the BIOMED-2 Concerted Action BMH4-CT98-3936. *Leukemia* 17: 2257–2317.
- Boyd, S. D., E. L. Marshall, J. D. Merker, J. M. Maniar, L. N. Zhang, B. Sahaf, C. D. Jones, B. B. Simen, B. Hanczaruk, K. D. Nguyen, et al. 2009. Measurement and clinical monitoring of human lymphocyte clonality by massively parallel VDJ pyrosequencing. *Sci. Transl. Med.* 1: 12ra23.
- Yaari, G., J. A. Vander Heiden, M. Uduman, D. Gadala-Maria, N. Gupta, J. N. Stern, K. C. O'Connor, D. A. Hafler, U. Laserson, F. Vigneault, and S. H. Kleinstein. 2013. Models of somatic hypermutation targeting and substitution based on synonymous mutations from high-throughput immunoglobulin sequencing data. *Front. Immunol.* 4: 358.
- Lefranc, M. P., C. Pommier, M. Ruiz, V. Giudicelli, E. Foulquier, L. Truong, V. Thouvenin-Contet, and G. Lefranc. 2003. IMGT unique numbering for immunoglobulin and T cell receptor variable domains and Ig superfamily V-like domains. *Dev. Comp. Immunol.* 27: 55–77.
- Wang, Y., K. J. Jackson, B. Gäeta, W. Pomat, P. Siba, W. A. Sewell, and A. M. Collins. 2011. Genomic screening by 454 pyrosequencing identifies a new human IGHV gene and sixteen other new IGHV allelic variants. *Immunogenetics* 63: 259–265.
- Watson, C. T., K. M. Steinberg, J. Huddleston, R. L. Warren, M. Malig, J. Schein, A. J. Willsey, J. B. Joy, J. K. Scott, T. A. Graves, et al. 2013. Complete haplotype sequence of the human immunoglobulin heavy-chain variable, diversity, and joining genes and characterization of allelic and copy-number variation. *Am. J. Hum. Genet.* 92: 530–546.
- Gadala-Maria, D., G. Yaari, M. Uduman, and S. H. Kleinstein. 2015. Automated analysis of high-throughput B-cell sequencing data reveals a high frequency of novel immunoglobulin V gene segment alleles. *Proc. Natl. Acad. Sci. USA* 112: E862–E870.
- Ye, J., N. Ma, T. L. Madden, and J. M. Ostell. 2013. IgBLAST: an immunoglobulin variable domain sequence analysis tool. *Nucleic Acids Res.* 41: W34–40.
- Lavinder, J. J., Y. Wine, C. Giesecke, G. C. Ippolito, A. P. Horton, O. I. Lungu, K. H. Hoi, B. J. DeKosky, E. M. Murrin, M. M. Wirth, et al. 2014. Identification and characterization of the constituent human serum antibodies elicited by vaccination. *Proc. Natl. Acad. Sci. USA* 111: 2259–2264.
- Willis, L. G., M. L. Winston, and B. M. Honda. 1992. Phylogenetic relationships in the honeybee (genus *Apis*) as determined by the sequence of the cytochrome oxidase II region of mitochondrial DNA. *Mol. Phylogenet. Evol.* 1: 169–178.
- Hill, M. O. 1973. Diversity and evenness—unifying notation and its consequences. *Ecology* 54: 427–432.
- Tuomisto, H. 2010. A diversity of beta diversities: straightening up a concept gone awry. Part 1. Defining beta diversity as a function of alpha and gamma diversity. *Ecography* 33: 2–22.
- Crotty, S., R. D. Aubert, J. Glidewell, and R. Ahmed. 2004. Tracking human antigen-specific memory B cells: a sensitive and generalized ELISPOT system. *J. Immunol. Methods* 286: 111–122.
- Holtmeier, W., A. Hennemann, and W. F. Caspary. 2000. IgA and IgM V<sub>H</sub> repertoires in human colon: evidence for clonally expanded B cells that are widely disseminated. *Gastroenterology* 119: 1253–1266.
- Yuvaraj, S., G. Dijkstra, J. G. Burgerhof, P. M. Dammers, M. Stoel, A. Visser, F. G. Kroese, and N. A. Bos. 2009. Evidence for local expansion of IgA plasma cell precursors in human ileum. *J. Immunol.* 183: 4871–4878.
- Lindner, C., B. Wahl, L. Föhse, S. Suerbaum, A. J. Macpherson, I. Prinz, and O. Pabst. 2012. Age, microbiota, and T cells shape diverse individual IgA repertoires in the intestine. *J. Exp. Med.* 209: 365–377.
- Thoree, V. C., S. J. Golby, L. Boursier, M. Hackett, D. K. Dunn-Walters, J. D. Sanderson, and J. Spencer. 2002. Related IgA1 and IgG producing cells in blood and diseased mucosa in ulcerative colitis. *Gut* 51: 44–50.
- von Büdingen, H. C., T. C. Kuo, M. Sirota, C. J. van Belle, L. Apeltsin, J. Glanville, B. A. Cree, P. A. Gourraud, A. Schwartzburg, G. Huerta, et al. 2012. B cell exchange across the blood-brain barrier in multiple sclerosis. *J. Clin. Invest.* 122: 4533–4543.
- Stern, J. N., G. Yaari, J. A. Vander Heiden, G. Church, W. F. Donahue, R. Q. Hintzen, A. J. Huttner, J. D. Laman, R. M. Nagra, A. Nylander, et al. 2014. B cells populating the multiple sclerosis brain mature in the draining cervical lymph nodes. *Sci. Transl. Med.* 6: 248ra107.
- Barone, F., A. Vossenkamper, L. Boursier, W. Su, A. Watson, S. John, D. K. Dunn-Walters, P. Fields, S. Wijetilleka, J. D. Edgeworth, and J. Spencer. 2011. IgA-producing plasma cells originate from germinal centers that are induced by B-cell receptor engagement in humans. *Gastroenterology* 140: 947–956.
- Bergqvist, P., A. Stenstrom, L. Hazanov, A. Holmberg, J. Mattsson, R. Mehr, M. Bemark, and N. Y. Lycke. 2013. Re-utilization of germinal centers in multiple Peyer's patches results in highly synchronized, oligoclonal, and affinity-matured gut IgA responses. *Mucosal Immunol.* 6: 122–135.
- MacLennan, I. C., K. M. Toellner, A. F. Cunningham, K. Serre, D. M. Sze, E. Zúñiga, M. C. Cook, and C. G. Vinuesa. 2003. Extrafollicular antibody responses. *Immunol. Rev.* 194: 8–18.
- Mesin, L., R. Di Niro, K. M. Thompson, K. E. Lundin, and L. M. Sollid. 2011. Long-lived plasma cells from human small intestine biopsies secrete immunoglobulins for many weeks in vitro. *J. Immunol.* 187: 2867–2874.
- Wu, Y. C., D. Kipling, and D. K. Dunn-Walters. 2011. The relationship between CD27 negative and positive B cell populations in human peripheral blood. *Front. Immunol.* 2: 81.